Slider block friction model for landslides: Application to Vaiont and La Clapière landslides

A. Helmstetter,[1,2] D. Sornette,[3,4,5] J.-R. Grasso,[1,6] J. V. Andersen,[3,7] S. Gluzman,[5] and V. Pisarenko[8]

Received 20 August 2002; revised 26 September 2003; accepted 29 October 2003; published 20 February 2004.

[1] Accelerating displacements preceding some catastrophic landslides have been found to display a finite time singularity of the velocity $v \sim 1/(t_c - t)$ [*Voight*, 1988a, 1988b]. Here we provide a physical basis for this phenomenological law based on a slider block model using a state- and velocity-dependent friction law established in the laboratory. This physical model accounts for and generalizes Voight's observation: Depending on the ratio B/A of two parameters of the rate and state friction law and on the initial frictional state of the sliding surfaces characterized by a reduced parameter X_i, four possible regimes are found. Two regimes can account for an acceleration of the displacement. For $B/A > 1$ (velocity weakening) and $X_i < 1$ the slider block exhibits an unstable acceleration leading to a finite time singularity of the displacement and of the velocity $v \sim 1/(t_c - t)$, thus rationalizing Voight's empirical law. An acceleration of the displacement can also be reproduced in the velocity-strengthening regime for $B/A < 1$ and $X_i > 1$. In this case, the acceleration of the displacement evolves toward a stable sliding with a constant sliding velocity. The two other cases ($B/A < 1$ and $X_i < 1$ and $B/A > 1$ and $X_i > 1$) give a deceleration of the displacement. We use the slider block friction model to analyze quantitatively the displacement and velocity data preceding two landslides, Vaiont and La Clapière. The Vaiont landslide was the catastrophic culmination of an accelerated slope velocity. La Clapière landslide was characterized by a peak of slope acceleration that followed decades of ongoing accelerating displacements succeeded by a restabilization. Our inversion of the slider block model in these data sets shows good fits and suggests a classification of the Vaiont landslide as belonging to the unstable velocity-weakening sliding regime and La Clapière landslide as belonging to the stable velocity-strengthening regime. *INDEX TERMS:* 3210 Mathematical Geophysics: Modeling; 8010 Structural Geology: Fractures and faults; 8020 Structural Geology: Mechanics; 8045 Structural Geology: Role of fluids; 8122 Tectonophysics: Dynamics, gravity and tectonics; *KEYWORDS:* landslides, friction law, rupture

Citation: Helmstetter, A., D. Sornette, J.-R. Grasso, J. V. Andersen, S. Gluzman, and V. Pisarenko (2004), Slider block friction model for landslides: Application to Vaiont and La Clapière landslides, *J. Geophys. Res.*, *109*, B02409, doi:10.1029/2002JB002160.

1. Introduction

[2] Landslides constitute a major geologic hazard in most parts of the world. The force of rocks, soil, or other debris moving down a slope can cause devastation. In the United States, landslides occur in most states, causing \$1–2 billion in damages and more than 25 fatalities on average each year. Costs and casualty rates are similar in the European Union and often have even more catastrophic impacts in developing countries. Landslides occur in a wide variety of geomechanical contexts and geological settings and as a response to various loading and triggering processes. They are often associated with other major natural disasters such as earthquakes, floods, and volcanic eruptions.

[3] Landslides can occur without discernible warning. There are, however, well-documented cases of precursory signals, showing accelerating slip over timescales of weeks to decades (see *Voight* [1978] for a review). While only a few such landslides have been monitored in the past,

[1]Laboratoire de Géophysique Interne et Tectonophysique, Observatoire de Grenoble, Université Joseph Fourier, Grenoble, France.
[2]Now at Institute of Geophysics and Planetary Physics, University of California, Los Angeles, California, USA.
[3]Laboratoire de Physique de la Matière Condensée, CNRS UMR 6622 and Université de Nice-Sophia Antipolis, Nice, France.
[4]Department of Earth and Space Sciences, University of California, Los Angeles, California, USA.
[5]Institute of Geophysics and Planetary Physics, University of California, Los Angeles, California, USA.
[6]Now at U.S. Geological Survey, Western Region Earthquake Hazards Team, Menlo Park, California, USA.
[7]U. F. R. de Sciences Economiques, Gestion, Mathématiques et Informatique, CNRS UMR7536 and Université Paris X-Nanterre, Nanterre, France.
[8]International Institute of Earthquake Prediction Theory and Mathematical Geophysics, Russian Academy of Science, Moscow, Russia.

0148-0227/04/2002JB002160$09.00

modern monitoring techniques are allowing a wealth of new quantitative observations based on GPS and synthetic aperture radar technology to map the surface velocity field [*Mantovani et al.*, 1996; *Fruneau et al.*, 1996; *Parise*, 2001; *Malet et al.*, 2002] and seismic monitoring of slide quake activity [*Gomberg et al.*, 1995; *Xu et al.*, 1996; *Rousseau*, 1999; *Caplan-Auerbach et al.*, 2001]. Derived from civil engineering methods, the standard approach to mapping a landslide hazard is to identify the conditions under which a slope becomes unstable [e.g., *Hoek and Bray*, 1997]. In this approach, geomechanical data and properties are inserted in finite or discrete element numerical codes to predict the distance to a failure threshold. The results of such analyses are expressed using a safety factor F, defined as the ratio of the maximum retaining force to the driving forces. According to this approach a slope becomes unstable when $F < 1$. By its nature, standard stability analysis does not account for acceleration in slope movement [e.g., *Hoek and Brown*, 1980] but gives an all-or-nothing value. In this view, any specific landslide is essentially unpredictable, and the focus is on the recognition of landslide-prone areas.

[4] To account for a progressive slope failure (i.e., a time dependence in stability analysis), previous researchers have taken a quasi-static approach in which some parameters are taken to vary slowly to account for progressive changes of external conditions and/or external loading. For instance, accelerated motions have been linked to pore pressure changes [e.g., *Vangenuchten and Derijke*, 1989; *Van Asch et al.*, 1999]. According to this approach an instability occurs when the gravitational pull on a slope becomes larger than the resistance of a particular subsurface level. This resistance is controlled by the friction coefficient of the interacting surfaces. Since pore pressure acts at the level of submicroscopic to macroscopic discontinuities, which themselves control the global friction coefficient, circulating water can hasten chemical alteration of the interface roughness, and pore pressure itself can force adjacent surfaces apart [*Vangenuchten and Derijke*, 1989]. Both effects reduce the friction coefficient, leading, when constant loading is applied, to accelerating movement. However, this approach does not forecast slope movements. Other studies proposed that (1) rates of slope movements are controlled by microscopic slow cracking and (2) when a major failure plane is developed, the abrupt decrease in shear resistance may provide a sufficiently large force imbalance to trigger a catastrophic slope rupture [*Kilburn and Petley*, 2003]. Such a mechanism, with a proper law of input of new cracks, may reproduce the acceleration preceding the collapse that occurred at Vaiont, Monte Toc, Italy [*Kilburn and Petley*, 2003].

[5] An alternative modeling strategy consists of viewing the accelerating displacement of the slope prior to the collapse as the final stage of the tertiary creep [*Saito and Uezawa*, 1961; *Saito*, 1965, 1969; *Kennedy and Niermeyer*, 1971; *Kilburn and Petley*, 2003]. Controlled experiments on landslides driven by a monotonic load increase at laboratory scale have been quantified by a scaling law relating the surface acceleration $d\dot{\delta}/dt$ to the surface velocity $\dot{\delta}$ according to

$$d\dot{\delta}/dt = A\dot{\delta}^{\alpha}, \tag{1}$$

where A and α are empirical constants [*Fukuzono*, 1985]. For $\alpha > 1$ this relationship predicts a divergence of the sliding velocity in finite time at some critical time t_c. The divergence is, of course, not to be taken literally: It signals a bifurcation from accelerated creep to complete slope instability for which inertia is no longer negligible. Several cases have been described with this relationship, usually for $\alpha = 2$, by plotting the time $t_c - t$ to failure as a function of the inverse of the creep velocity (for a review, see *Bhandari* [1988]). Indeed, integrating equation (1) gives

$$t_c - t \sim \left(\frac{1}{\dot{\delta}}\right)^{\frac{1}{\alpha-1}}. \tag{2}$$

These fits suggest that it might be possible to forecast impending landslides by recording accelerated precursory slope displacements. Indeed, for the Monte Toc, Vaiont landslide revisited here, *Voight* [1988b] mentioned that a prediction of the failure date could have been made more than 10 days before the actual failure by using a linear relation linking the inverse velocity and the time to failure, as found from equation (2) for $\alpha = 2$. *Voight* [1988b, 1989] proposed that the relation (1), which generalizes damage mechanics laws [*Rabotnov*, 1969; *Gluzman and Sornette*, 2001], can be used with other variables (including strain and/or seismic energy release) for a large variety of materials and loading conditions. Expression (1) seems to apply as well to diverse types of landslides occurring in rock and soil, including first-time and reactivated slides [*Voight*, 1988b]. Recently, such time-to-failure laws have been interpreted as resulting from cooperative critical phenomena and have been applied to the prediction of failure of heterogeneous composite materials [*Anifrani et al.*, 1995] and to precursory increase of seismic activity prior to main shocks [*Sornette and Sammis*, 1995; *Jaume and Sykes*, 1999; *Sammis and Sornette*, 2002].

[6] In this work, we develop a simple model of sliding instability based on the rate- and state-dependent friction law, which can rationalize the empirical time-to-failure laws proposed for landslides by *Voight* [1988b, 1989]. This rate and state friction law has been shown to lead to an asymptotic time-to-failure power law with $\alpha = 2$ in the late stage of frictional sliding motion between two solid surfaces preceding the elastodynamic rupture instability [*Dieterich*, 1992]. In addition, this model also describes the stable sliding regime, the situation where the time-to-failure behavior is absent. The rate and state fiction law has been established by numerous laboratory experiments (see, for instance, *Scholz* [1990, 1998], *Marone* [1998], and *Gomberg et al.* [2000] for reviews). The sliding velocities used in the laboratory to establish the rate and state friction laws are of the same order, 10^{-4}–10^{2} μm/s, as those observed for landslides before catastrophic collapse. State- and velocity-dependent friction laws have been developed and used extensively to model the preparatory and elastodynamical phases of earthquakes. In addition, analogies between landslide faults and tectonic faults have been noted [*Gomberg et al.*, 1995]. *Chau* [1995, 1999] first developed this analogy and used the rate and state friction law to model landslides and their precursory behavior. Chau transformed the problem into a formal nonlinear stability analysis of the type found in mathematical theory of dynamical systems, but no comparison with empirical data was presented. In addition and in contrast with the present work, Chau's analysis does not mention the existence of the finite

time singular precursory behavior, which signals the time of the dynamical instability of the landslide.

[7] We should stress that it is extremely difficult to obtain all relevant geophysical parameters that may be germane to a given landslide instability. Furthermore, it is also a delicate exercise to scale up laboratory results to the scale of mountain slopes. Having said that, probably the simplest model of landslides considers the moving part of the landslide as a block sliding over a surface. We test how the friction law of a rigid block driven by a constant gravity force can be useful for understanding the apparent transition between slow stable sliding and fast unstable sliding leading to slope collapse. Within such a conceptual framework the complexity of the landsliding behavior emerges from (1) the dynamics of the block behavior, (2) the dynamics of interactions between the block and the substratum, and (3) the history of the external loading (e.g., rain, earthquake).

[8] Previous efforts at modeling landslides in terms of a rigid slider block have taken either a constant friction coefficient or a slip- or velocity-dependent friction coefficient between the rigid block and the surface. A constant solid friction coefficient (Mohr-Coulomb law) is often taken to simulate bed over bedrock sliding. *Heim* [1932] proposed this model to forecast extreme runout length of rock avalanches. In contrast, a slip-dependent friction coefficient model is taken to simulate the yield-plastic behavior of a brittle material beyond the maximum of its strain-stress characteristics. For rock avalanches, *Eisbacher* [1979] suggested that the evolution from a static to a dynamic friction coefficient is induced by the emergence of a basal gouge. Studies using a velocity-dependent friction coefficient have mostly focused on the establishment of empirical relationships between shear stress τ and block velocity v, such as $v \sim \exp(a\tau)$ [*Davis et al.*, 1990] or $v \sim \tau^{1/2}$ [*Korner*, 1976] with, however, no definite understanding of the possible mechanism [see, e.g., *Durville*, 1992].

[9] In this work, we focus on two case studies, La Clapière sliding system in the French Alps and the Vaiont landslide in the Italian Alps. The latter landslide led to a catastrophic collapse after 70 days of recorded velocity increase. In the former case, decades of accelerating motion abated and gave way to a slowdown of the system. In section 2 we derive the different sliding regimes of this model, which depend on the ratio B/A of two parameters of the rate and state friction law and on the initial conditions of the reduced state variable. Sections 3 and 4 analyze the Vaiont and La Clapière landslides, respectively. We calibrate the slider block model to the two landslides and invert the key parameters. Our results suggest that the Vaiont landslide belongs to the velocity-weakening unstable regime, while La Clapière landslide is found to be in the stable strengthening sliding regime. Conclusions are presented in section 5. *Sornette et al.* [2004] investigate the potential of our present results for landslide prediction, using different methods to investigate the predictability of the failure times and prediction horizons.

2. Slider Block Model With State- and Velocity-Dependent Friction

2.1. Basic Formulation

[10] Following *Heim* [1932], *Korner* [1976], *Eisbacher* [1979], *Davis et al.* [1990], and *Durville* [1992], we model a landslide as a block resting on an inclined slope forming an angle ϕ with respect to the horizontal. In general, the solid friction coefficient μ between two surfaces is a function of the cumulative slip δ and of the slip velocity $\dot{\delta}$. We use the version of the rate and state friction law known as the Dieterich-Ruina or ''slowness'' law [*Dieterich*, 1978; *Ruina*, 1983], which is expressed as

$$\mu = \mu_0 + A \ln \frac{\dot{\delta}}{\dot{\delta}_0} + B \ln \frac{\theta}{\theta_0}, \tag{3}$$

where the state variable θ is usually interpreted as being proportional to the surface of contact between asperities. Here μ_0 is the friction coefficient for a sliding velocity $\dot{\delta}_0$ and a state variable θ_0. The state variable θ evolves with time according to

$$\frac{d\theta}{dt} = 1 - \frac{\theta \dot{\delta}}{D_c}, \tag{4}$$

where D_c is a characteristic slip distance, usually interpreted as the typical size of asperities. The friction law (3) with (4) accounts for the fundamental properties of a broad range of surfaces in contact, namely, that they strengthen logarithmically when aging at rest and weaken (rejuvenate) when sliding [*Scholz*, 1998].

[11] Expression (4) can be rewritten as

$$\frac{d\theta}{d\delta} = \frac{1}{\dot{\delta}} - \frac{\theta}{D_c}. \tag{5}$$

As reviewed by *Scholz* [1998], the friction at steady state is

$$\mu_S = \hat{\mu}_0 + (A - B) \ln \frac{\dot{\delta}}{\dot{\delta}_0}, \tag{6}$$

where $\hat{\mu}_0 = \mu_0 + B \ln (D_c/\theta_0 \dot{\delta}_0)$. Thus the derivative of the steady state friction coefficient with respect to the logarithm of the reduced slip velocity is $A - B$. If $A > B$, this derivative is positive: Friction increases with slip velocity, and the system is stable as more resistance occurs, which tends to react against the increasing velocity. In contrast, for $A < B$, friction exhibits the phenomenon of velocity weakening and is unstable. The primary parameter that determines stability, $A - B$, is a material property. For instance, for granite, $A - B$ is negative at low temperatures and becomes positive for temperatures above $\sim$300°C. In general, for low-porosity crystalline rocks the transition from negative to positive $A - B$ corresponds to a change from elastic-brittle deformation to crystal plasticity in the micromechanics of friction [*Scholz*, 1998]. For landslide application we note that sliding surfaces are usually lined with wear detritus, called cataclastic or fault gouge. The shearing of such granular materials involves an additional hardening mechanism (involving dilatancy), which tends to make $A - B$ more positive. For such materials, $A - B$ is positive when the material is poorly consolidated but decreases at elevated pressure and temperature as the material becomes lithified [see also *Scholz*, 1990, section 2.4]. While A is always found to be positive in laboratory experiments, negative B values are sometimes found [*Blanpied et al.*, 1995]. This rather special case

corresponds to a friction coefficient decreasing with the increase of the surface of contacts.

[12] In our model, a mountain flank is schematically represented, made of a block and a basal surface on which it is encased. The block represents the part of the slope which may be potentially unstable. For a constant gravity loading, the two parameters controlling the stability of the block are the dip angle ϕ between the surface on which the block stands and the horizontal and the solid friction coefficient μ. The block exerts stresses that are normal (σ) as well as tangential (τ) to this surface of contact. The angle ϕ controls the ratio of the shear over normal stress: $\tan\phi = \tau/\sigma$. As a first step we assume for simplicity that the usual solid friction law $\tau = \mu\sigma$ holds for all times, expressing that the shear stress τ exerted on the block is proportional to the normal stress with a coefficient of proportionality defining the friction coefficient μ. This assumption expresses a constant geometry of the block and of the surface of sliding. For the two landslides that we study in this paper, a rigid block sliding on a slope with a constant dip angle is a good first-order approximate of their behaviors. Within this conceptual model the complexity of the landsliding behavior emerges from the friction law. This first-order analysis neglects any possible complexity inherent either in the geometry and rheology of a larger set of blocks, in the substratum, or in the history of the external loading (e.g., earthquakes, rainfalls). Let us stress that our model does not describe the final instability associated with the runoff and is thus distinct from the studies of *Heim* [1932] and *Campbell* [1989], which do not describe as we do the initiation of a catastrophic collapse.

2.2. Solution of the Dynamical Equation

2.2.1. Asymptotic Power Law Regime for $B > A$

[13] As the sliding accelerates, the sliding velocity becomes sufficiently large such that $\dot{\delta} \gg D_c/\theta$, and we can neglect the first term $1/\dot{\delta}$ in the right-hand side of equation (5) [*Dieterich*, 1992]. This yields

$$\theta = \theta_0 \exp(-\delta/D_c), \tag{7}$$

which means that θ evolves toward zero. The friction law then reads

$$\frac{\tau}{\sigma} = \mu_0 + A \ln\frac{\dot{\delta}}{\dot{\delta}_0} - \frac{B\delta}{D_c}, \tag{8}$$

where we have inserted equation (7) into equation (3). In equation (8), τ and σ result from the mass of the block and are constant. The solution of equation (8) is [*Dieterich*, 1992]

$$\delta(t) = -\frac{AD_c}{B} \ln\left[\frac{B\dot{\delta}_0 \exp\left[\frac{\frac{\tau}{\sigma}-\mu_0}{A}\right]}{AD_c}(t_c - t)\right], \tag{9}$$

where t_c is determined by the initial condition $\delta(t = 0) \equiv \delta_i$:

$$t_c = \frac{AD_c}{B\dot{\delta}_0} \exp\left[-\left(\frac{B\delta_i}{AD_c} + \frac{\frac{\tau}{\sigma}-\mu_0}{A}\right)\right]. \tag{10}$$

The logarithmic blowup of the cumulative slip in finite time is associated with the divergence of the slip velocity

$$\dot{\delta} = \frac{AD_c}{B}\frac{1}{t_c - t}, \tag{11}$$

which recovers equation (2) for $\alpha = 2$.

2.2.2. Complete Solution and Synthesis of the Different Regimes

[14] Equation (9) is valid only for $B > A$ and for t sufficiently close to t_c, for which the slip velocity $\dot{\delta}$ is large, ensuring the validity of the approximation leading to equation (7). However, even in the unstable case $B > A$, the initiation of sliding cannot be described by using the approximation established for t close to t_c and requires a description different from equations (9) and (11). Furthermore, we are interested in different situations, in which the sliding may not always result in a catastrophic instability (e.g., La Clapière), a situation which can be interpreted as the stable regime $B < A$.

[15] The sliding block displays different regimes as a function of the friction law parameters and of the initial conditions, i.e., the ratio B/A, where A and B are defined in equation (3), and the initial value X_i of the reduced state variable X defined by equation (A4) in Appendix A. The variable X is proportional to the state variable θ, describing the duration of contacts between asperities. The proportional factor between X and θ is such that the initial value $X_i = 1$ is the limit between the stable and the unstable regime. The complete solution in the different regimes is derived in Appendix A, is illustrated in Figure 1, and is summarized below and in Table 1.

[16] 1. For $0 < B/A < 1$ the sliding is always stable. Depending on the initial value at $t = 0$ of the reduced state variable X_i, the sliding velocity either increases (if $X_i > 1$) or decreases (if $X_i < 1$) toward a constant value.

[17] 2. For $B/A > 1$ the sliding is always unstable. When $X_i < 1$ the sliding velocity increases toward a finite time singularity. The slip velocity diverges as $1/(t_c - t)$, corresponding to a logarithmic singularity of the cumulative slip. For $X_i > 1$ the velocity decreases toward a vanishingly small value.

[18] 3. For $B = A$ the state variable either decreases (for $S\theta_0 > 1$) or increases (for $S\theta_0 < 1$) linearly as a function of time, where S is defined by equation (A2) and depends on the material properties but not on the initial conditions. In the former case this retrieves a finite time singularity with the slip velocity diverging as $1/(t_c - t)$. In the latter case the slip velocity decreases as $\dot{\delta} \sim 1/t$ at large times. The case $B = A$ is fundamentally different in its independence with respect to the initial conditions.

2.3. Analysis of Landslide Observations

[19] In this section we test how the model can reproduce the observed acceleration of the displacement for the Vaiont and La Clapière landslides. The Vaiont landslide was the catastrophic culmination of an accelerated slope velocity over a 2-month period [*Muller*, 1964]. La Clapière landslide was characterized by a long-lasting acceleration that peaked in the 1986–1988 period, succeeded by a restabilizing phase [*Susella and Zanolini*, 1996]. An acceleration of the displacement can arise from the friction model

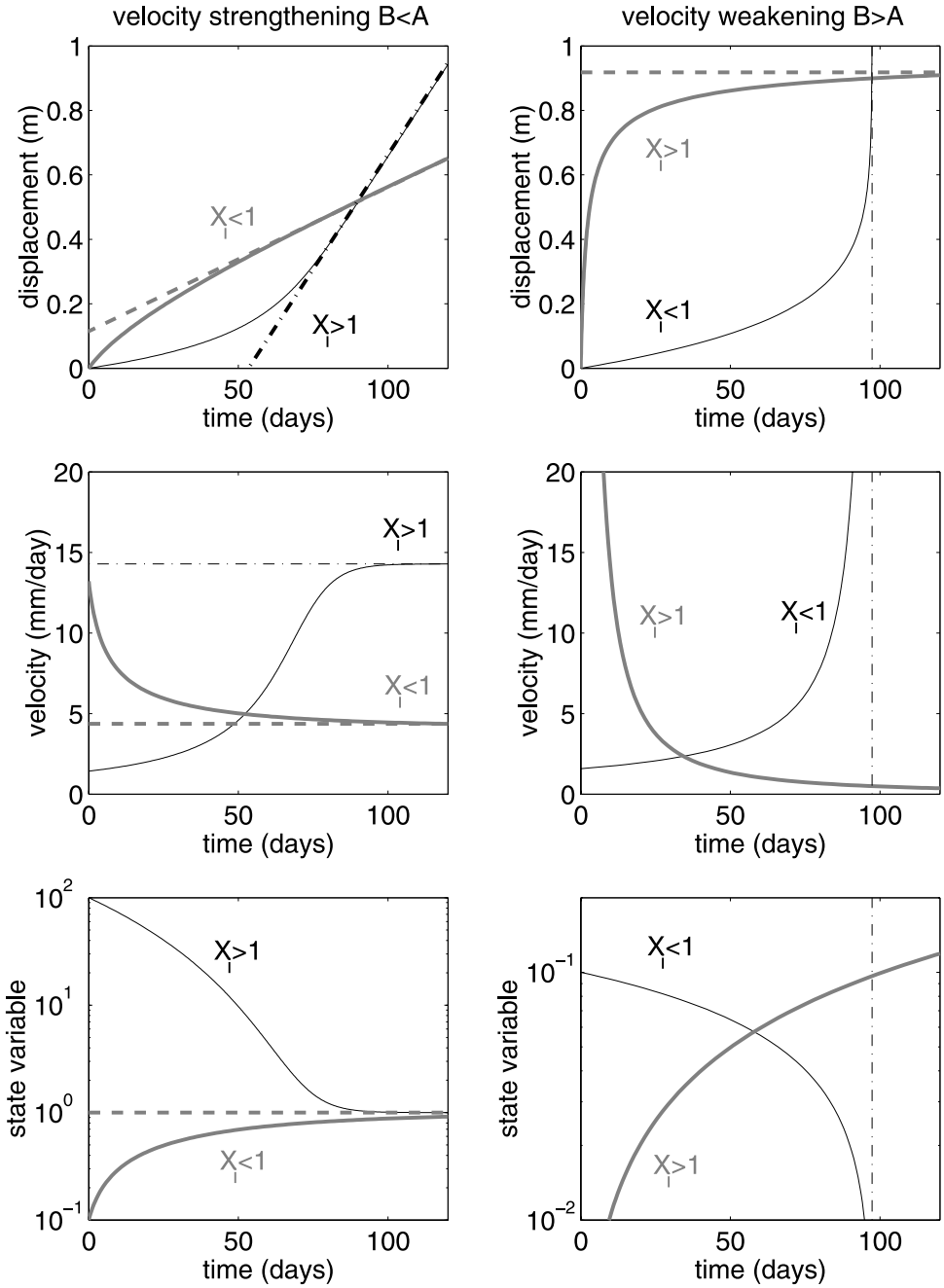

Figure 1. Schematic classification of the different regimes of sliding discussed in the text: (left) stable regime $B < A$ and (right) unstable regime $B > A$. In each case the displacement, velocity, and state variables are shown as a function of time. Each regime (stable and unstable) is divided into two cases, depending on the dimensionless initial value $X_i \propto \theta_i$ of the state variable. The thick solid curves correspond to decreasing velocities and increasing state variables. The thin solid curves correspond to increasing velocities and decreasing state variables. See color version of this figure in the HTML.

in two regimes, either in the stable regime with $B > A$ and $X_i > 1$ or in the unstable regime with $B < A$ and $X_i < 1$. However, these two regimes are very similar in the early time regime before the critical time (see Figure 1). With only limited data it is therefore very difficult to distinguish the regime a landslide is in. We invert the friction law parameters from the velocity and displacement data of the Vaiont and La Clapière landslides. Our goal is to test if this model is useful for distinguishing an unstable accelerating

Table 1. Synthesis of the Different Slip Regimes as a Function of the Ratio B/A Defined in Equation (3) and of the Initial Value X_i of the Reduced State Variable Defined in Equation (A4)[a]

	$X_i < 1$	$X_i > 1$
$B/A > 1$	FTS (9), (10), (11)	power law plasticity hardening (A11)
$0 < B/A < 1$	θ decreases, $\dot{\delta}$ increases	θ increases, $\dot{\delta}$ decreases
$B/A < 0$	θ decreases, $\dot{\delta}$ decreases	θ increases, $\dot{\delta}$ increases

[a]FTS stands for "finite time singularity." Numbers in parentheses refer to equation numbers.

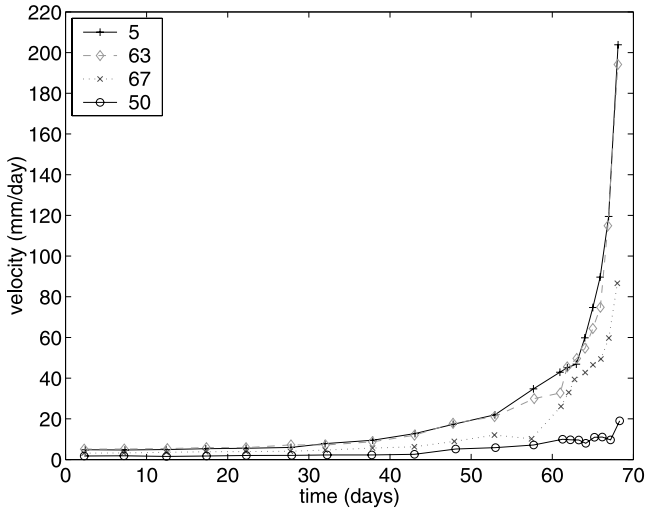

Figure 2. Velocity measurements for the four bench marks of the Vaiont landslide. Bench marks 5 and 63 exhibit similar acceleration. Bench mark 50 shows only a relatively small acceleration in absolute values at the end of the 60-day accelerating phase. Its acceleration is, however, significant in relative values, as seen in Figure 4. Data are from *Muller* [1964]. See color version of this figure in the HTML.

sliding characterized by $B > A$ from a stable accelerating regime occurring for $B < A$.

3. Vaiont Landslide

3.1. Historical and Geomechanical Overview

[20] On 9 October 1963 on the Monte Toc slope in the Dolomite region of the Italian Alps ~100 km north of Venice, a 2-km-wide landslide was initiated at an elevation of 1100–1200 m. This is 500–600 m above the valley floor. The event ended 70 days later in a 20 m/s runaway of ~0.3 km^3 of rocks sliding into a dam reservoir. The high velocity of the slide triggered a water surge within the reservoir, overtopping the dam and killing 2500 people in the villages (Longarone, Pirago, Villanova, Rivalta, and Fae) downstream. The landslide occurred on the mountain above a newly built reservoir. The first attempt to fill up the reservoir was made between March and November 1960. It induced recurrent observations of creeping motions of a large mass of rock above the reservoir and led to several small and rather slow slides [*Muller*, 1964]. Lowering the reservoir water level induced the rock mass velocities to drop from ~40 to <1 mm/d. A controlled raising of the water level and cycling were performed. A second peak of creeping velocity, at ~10 mm/d, was induced by the 1962 filling cycle. The 1963 filling cycle started in April. From May, recurrent increases of the creep velocity were measured using four bench marks. On 26 September 1963, lowering the reservoir level was again initiated. Contrary to what happened in 1960 and again in 1962, the velocities continued to increase at an increasing rate. This culminated in the 20 m/s downward movement of a volume of 0.3 km^3 of rock in the reservoir.

[21] The landslide geometry is a rough rectangular shape 2 km wide and 1.3 km in length. Velocity measurements are available for four bench marks, corresponding to four different positions on the mountain slope, denoted 5, 50, 63, and 67 in the Vaiont nomenclature. Bench marks 63 and 67 are located at the same elevation in the upper part of the landslide a few hundred meters from the submittal scarp. The distance between the two bench marks is 1.1 km. Bench marks 5 and 50 are 700 m downward from the 63–67 bench mark level. Figure 2 shows the velocity of the four bench marks as a function of time prior to the Vaiont landslide. For these four bench marks the deformation of the sliding zone prior to rupture is not homogeneous, as the cumulative displacement in the period from 2 August 1963 to 8 October 1963 ranges from 0.8 to 4 m. However, the low degree of disintegration of the distal deposit [*Erismann and Abele*, 2000] argues for a possible homogeneous block behavior during the 1963 sliding collapse.

[22] It was recognized later that limestones and clay beds dipping into the valley provide conditions favorable for dip-slope failures [*Muller*, 1964, 1968; *Broili*, 1967]. There is now a general agreement on the collapse history of the 1963 Vaiont landslide [see, e.g., *Erismann and Abele*, 2000]. The failure occurred along bands of clays within the limestone mass at depths between 100 and 200 m below the surface [*Hendron and Patton*, 1985]. Raising the reservoir level increased water pore pressure in the slope flank, which triggered failure in the clay layers. Final sliding occurred after 70 days of downslope accelerating movement. The rock mass velocity progressively increased from 5 mm/d to more than 20 cm/d, corresponding to a cumulative displacement of a few meters over this 70-day period [*Muller*, 1964].

3.2. Analysis of the Velocity Data With the Slider Block Model Parameters

[23] Figure 3 shows the inverse of the velocity shown in Figure 2 to test the finite time singularity hypothesis (equations (2) and (11)). Note that Figure 3 does not require knowledge of the critical time t_c and is not a fit to the data.

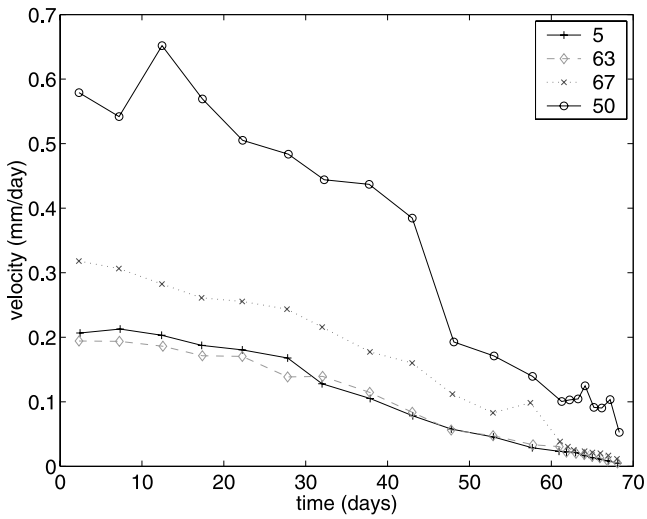

Figure 3. Same as Figure 2 but plotting the inverse of the velocity as time t. All curves are roughly linear, showing that the velocity exhibits a finite time singularity $v \sim 1/(t_c - t)$ with $t_c \approx 69.5$ days for all bench marks, estimated as the intercept of the extrapolation of these curves with the horizontal axis. See color version of this figure in the HTML.

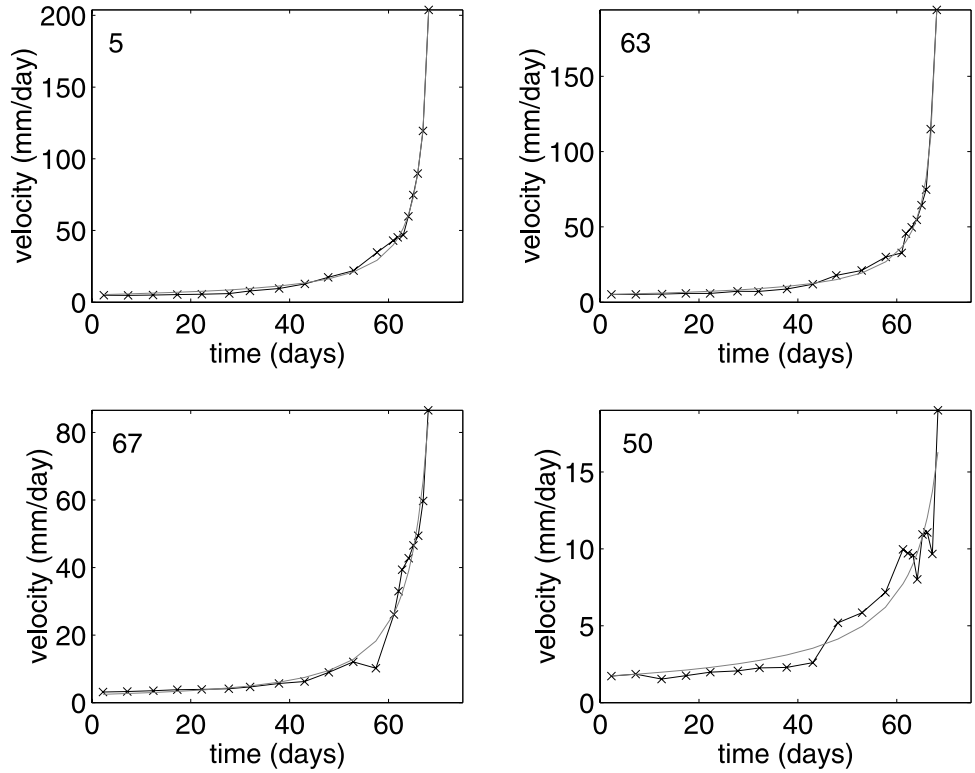

Figure 4. For each of the four Vaiont bench marks the velocity data of Figure 2 are fitted with the slider block model with the state and velocity friction law (A7) and (A6) by adjusting the set of parameters B/A, D, and T and the initial condition of the state variable X_i. The data are shown as the crosses linked by straight segments, and the fit is the thin line. See color version of this figure in the HTML.

The curves for all bench marks are roughly linear in this representation, in agreement with a finite time singularity of the velocity (equation (2)) with $\alpha = 2$. It was the observations presented in Figure 3 that led *Voight* [1988b] to suggest that a prediction could have been issued more than 10 days before the collapse. We note that the law $\dot{\delta} \propto 1/(t_c - t)$ requires the adjustment of α to the special value 2 in the phenomenological approach [*Voight*, 1988b] underlying equation (2), while it is a robust and universal result in our model in the velocity-weakening regime $B > A$ and for a normalized initial state variable larger than 1 (see equation (11) and Table 1).

[24] In order to invert the parameters B/A, D, and T defined in equations (A6) and (A8) of the friction model and the initial condition of the state variable X_i from the velocity data, we minimize the RMS of the residual between the observed velocity $\dot{\delta}_{\mathrm{obs}}$ and the velocity $\dot{\delta}$ from the friction model (equations (A7) and (A6)). The parameters D and T are complex functions of the parameters of the friction law that have no clear physical meaning. The constant D in equation (A6) is obtained by taking the derivative of the RMS with respect to D, which yields

$$D = \frac{\sum_{t_i} \dot{\delta}(t_i)\dot{\delta}_{\mathrm{obs}}(t_i)}{\sum_{t_i} \dot{\delta}(t_i)^2}, \qquad (12)$$

where the velocity $\dot{\delta}$ in equation (12) is evaluated for $D = 1$ in equation (A6). We use a simplex algorithm (Matlab subroutine) to invert the three other parameters B/A, T, and X_i. For each data set we use different starting points (initial parameter values for the simplex algorithm) in the inversion to test for the sensitivity of the results on the starting point.

[25] Figure 4 shows the fits to the velocity data using the slider block model with the state and velocity friction law (equations (A6) and (A7)). The values of B/A are 1.35 (bench mark 5), 1.24 (bench mark 63), 0.99 (bench mark 67), and 1.00001 (bench mark 50). Most values are larger than or equal to 1, which is compatible with the finite time singularity regime summarized in Table 1. The parameters of the friction law are very poorly constrained by the inversion. In particular, even for those bench marks where the best fit gives $B > A$, other models with $B < A$ provide a good fit to the velocity with only slightly larger RMS.

[26] Figure 5 gives another representation of Figure 4, showing the inverse of the velocity as a function of time. The increase of velocity abates before the critical time for all bench marks, which may explain the values $B < A$ sometimes obtained by the inversion.

4. La Clapière Landslide: Aborted 1982–1987 Acceleration

[27] We now report results on another case which exhibited a transient acceleration followed by a restabilization. This provides an example of the $B < A$ stable slip regime, as interpreted within the friction model.

4.1. Historical and Geomechanical Overview

4.1.1. Geomechanical Setting and Displacement History: 1950–2000

[28] La Clapière landslide is located at an elevation between 1100 and 1800 m on a 3000-m-high slope. The

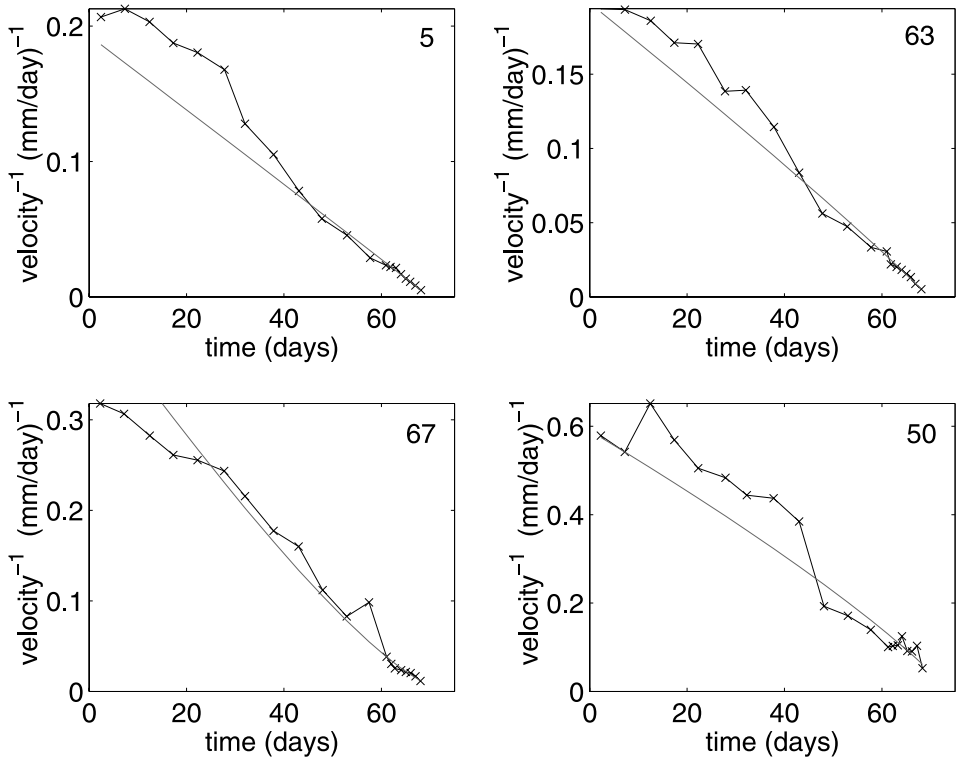

Figure 5. Same as Figure 4 but showing the inverse of the velocity. The upward bending of the curve for bench mark 67 reflects the saturation of the velocity in the stable regime $B < A$. The fit for the three other bench marks characterized by $B \geq A$ is very close to the asymptotic solution $v \sim 1/(t_c - t)$ (equation (11)). See color version of this figure in the HTML.

landslide has a width of ~1000 m. Figure 6 shows La Clapière landslide in 1979 before the acceleration of the displacement and in 1999 after the end of the crisis. The volume of mostly gneiss rocks in the landslide is estimated to be $\sim 50 \times 10^6$ m^3. At an elevation of ~1300 m an 80-m-thick bed provides a more massive and relatively stronger level compared with the rest of the relatively weak and fractured gneiss. The two lithological entities are characterized by a change in mica content which is associated with a change of the peak strength and of the elastic modulus by a factor of 2 [*Follacci et al.*, 1988, 1993]. Geomorphological criteria allow three distinct subentities within the landslide to be distinguished: NW, central, and SW [*Follacci et al.*, 1988].

[29] There is some historical evidence that the rock mass started to be active before the beginning of the twentieth century. In 1938, photographic documents attest to the existence of a scarp at 1700 m elevation [*Follacci*, 2000]. In the 1950–1980 period, triangulation and aerial photogrametric surveys provide constraints on the evolution of the geometry and the kinematics of the landslide (Figure 7). The displacement rate measured by aerial photogrammetric survey increased from 0.5 m/yr in the 1950–1960 period to 1.5 m/yr in the 1975–1982 period [*Follacci et al.*, 1988]. Starting in 1982, the displacements of 43 bench marks have been monitored on a monthly basis using distance meters (a motorized theodolite (TM300) and a Wild DI 3000 distance meter) [*Follacci et al.*, 1988, 1993; *Susella and Zanolini*, 1996]. The displacement data for the five bench marks shown in Figure 6 are represented in Figure 8. The velocity of bench mark 10, which is typical, is shown in Figure 9. The rock mass velocities exhibited a dramatic increase between January 1986 and January 1988, culminating in the 80 mm/d velocity during summer 1987 and 90 mm/d in October 1987. The similarity of bench mark trajectories and the synchronous acceleration phase for most bench marks attest to a global deep-seated behavior of this landslide [e.g., *Follacci et al.*, 1988]. However, a partitioning of deformation occurred, as reflected by the difference in absolute values of bench mark displacements (Figure 8). The upper part of the landslide moved slightly faster than the lower part and the NW block. The observed decrease in displacement rate since 1988 attests to a change in landsliding regime at the end of 1987 (Figure 8).

4.1.2. Correlations Between the Landslide Velocity and the River Flow

[30] The landslide velocity displays large fluctuations correlated with fluctuations of the river flow in the valley as shown in Figure 9. There is a seasonal increase of the slope velocity, which reaches a maximum $V_{max} \leq 30$ mm/d. The slope velocity increases in the spring because of snowmelt and over a few days after heavy precipitation concentrated in the fall of each year [*Follacci et al.*, 1988; *Susella and Zanolini*, 1996]. During the 1986–1988 period the snowmelt and rainfalls were not anomalously high, but the maximum value of the velocity, $V_{max} = 90$ mm/d, was much larger than the velocities reached during the 1982–1985 period for comparable rainfalls and river flows [*Follacci et al.*, 1988, 1993]. This strongly suggests that the hydrological conditions are not the sole control param-

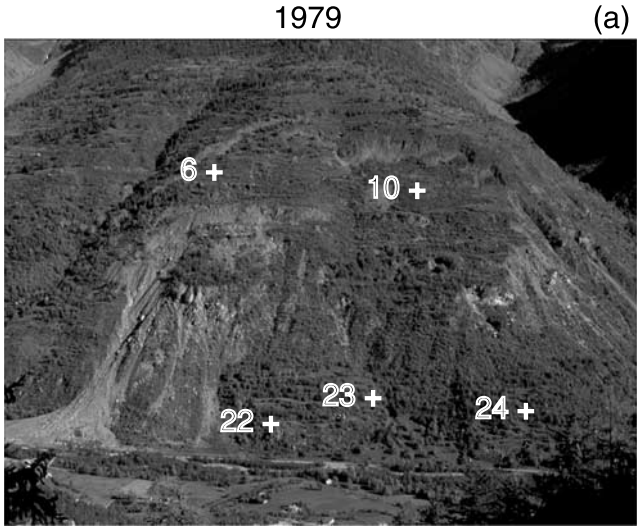

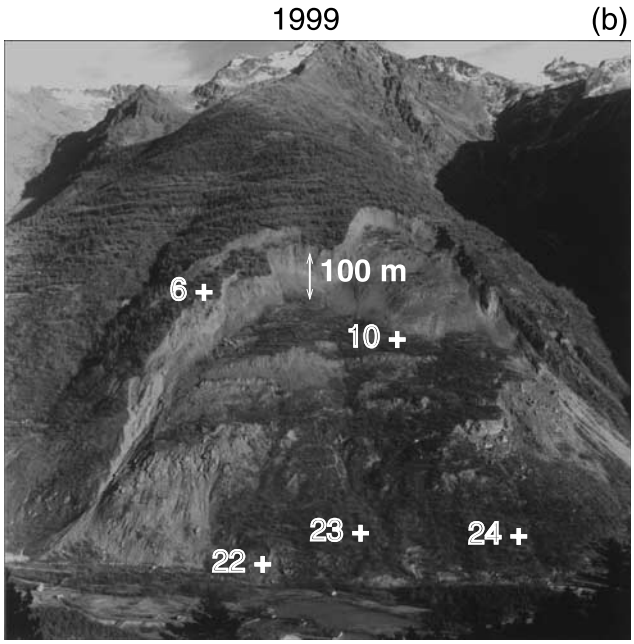

Figure 6. (a) Photograph of La Clapière landslide taken in 1979. The volume of mostly gneiss rocks implied in the landslide is estimated to be $\sim 50 \times 10^6$ m^3. The summit scarps are not connected. The photograph also shows the locations of all the bench marks that have been monitored since the end of 1982. (b) Photograph of La Clapière landslide taken in 1999. The overall surface pattern is preserved. The main feature related to the 1982–1988 crisis is a new summit scarp with a total displacement of $\sim$100 m in 1999, indicated by the arrow.

eters explaining both the strong 1986–1987 acceleration and the equally strong slowdown in 1988–1990. During the interval 1988–1990 the monthly recorded velocities slowed down to a level slightly higher than the pre-1986 values. Since 1988 the seasonal variations of the average velocity never recovered the level established during the 1982–1985 period [*Follacci et al.*, 1993; *David*, 2000]. *Rat* [1988]

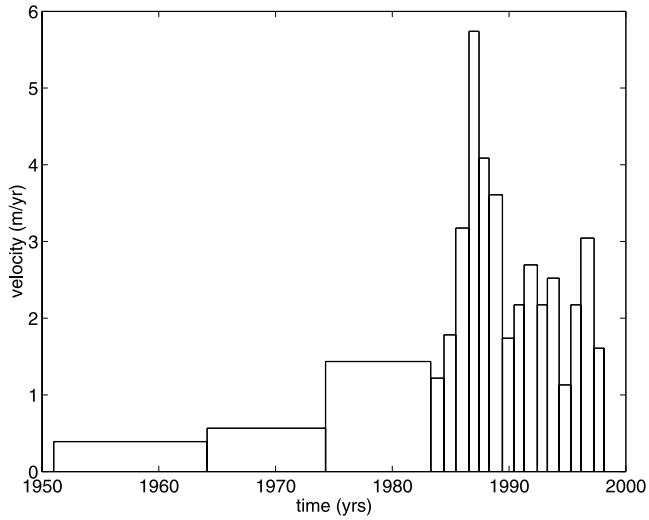

Figure 7. Velocity of the landslide of La Clapière mount over almost 50 years, showing that the dangerous velocity peak in 1987 was preceded by a progressive buildup extending over several decades. Before 1982 the velocity was inferred from aerial photographs in 1951, 1964, 1974, and 1982. After 1982 the velocity is obtained from automated triangulation and geodesy. Data are from *Centre Etudes Techniques de l'Equipement* (*CETE*) [1999].

derives a relationship between the river flow and the landslide velocity by adjusting a hydrological model to the velocity data in the period 1982–1986. This model tuned to this time period does not reproduce the observed acceleration of the velocity after 1986.

4.1.3. Fracturing Patterns Contemporary to the 1986–1987 Accelerating Regime

[31] In 1985–1986 a transverse crack initiated in the upper part of the NW block. It reached 50 m of vertical offset in 1989. The maximum rate of change of the fracture size and of its opening occurred in 1987 [*Follacci et al.*, 1993]. This new

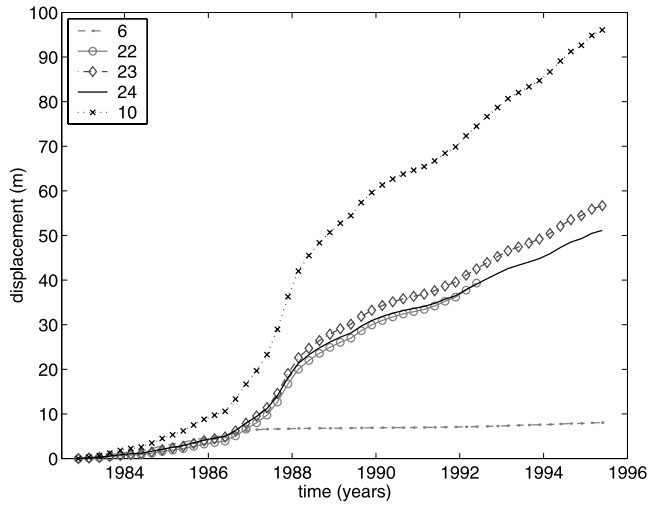

Figure 8. Displacement for the five bench marks on La Clapière site shown in Figure 6. See color version of this figure in the HTML.

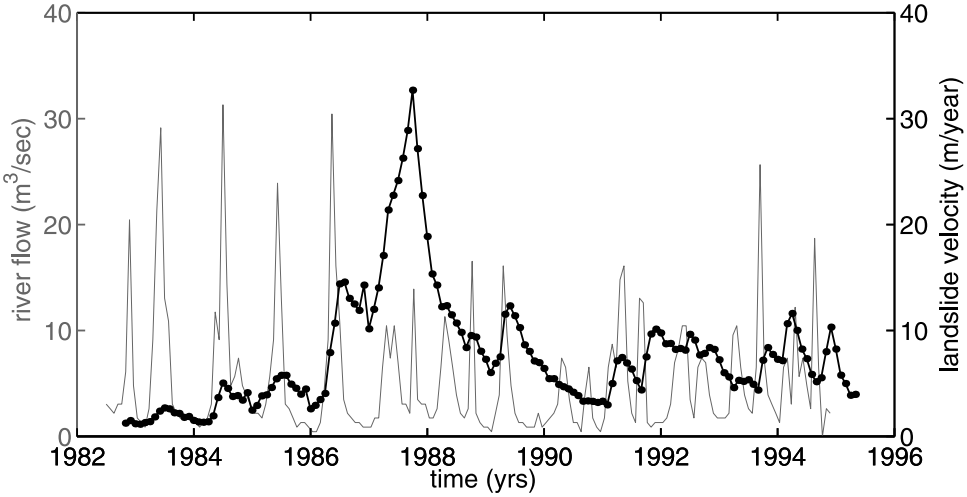

Figure 9. Velocity pattern for bench mark 10 of La Clapière landslide (thick curve and dots) and flow rates of the Tinée River (thin curve) during the 1982–1995 period. Because the Tinée River runs at the base of La Clapière landslide, the river flow rate reflects the water flow within the landslide [*Follacci et al.*, 1993; *Susella and Zanolini*, 1996]. The flow rates are measured at St. Etienne village, 2 km upstream from the landslide site. There is no stream network on the landslide site. The Tinée flow drains a 170 km^2 basin. This tiny basin is homogeneous in terms of both slopes and elevation (in the 1000–3000 m range). Accordingly, the seasonal fluctuations of the river flow reflect the amount of water within the landslide slope from rainfall and snowmelt. Data are from *Centre Etudes Techniques de l'Equipement (CETE)* [1996]. See color version of this figure in the HTML.

transverse crack uncoupled the NW block from the upper part of the mountain, which moved at a much smaller velocity below 1 mm/d since 1985–1986 [*Follacci et al.*, 1993] (Figures 6 and 10). Since summer 1988 a homogenization of the surface morphological faces and a regression of the main summit scarp were reported. The regression of the summit scarp was observed as a new crack started to open in September 1988. Its length increased steadily to reach 500 m, and its width reached 1.75 m in November 1988. Accordingly, the new elevation of the main scarp in the SE

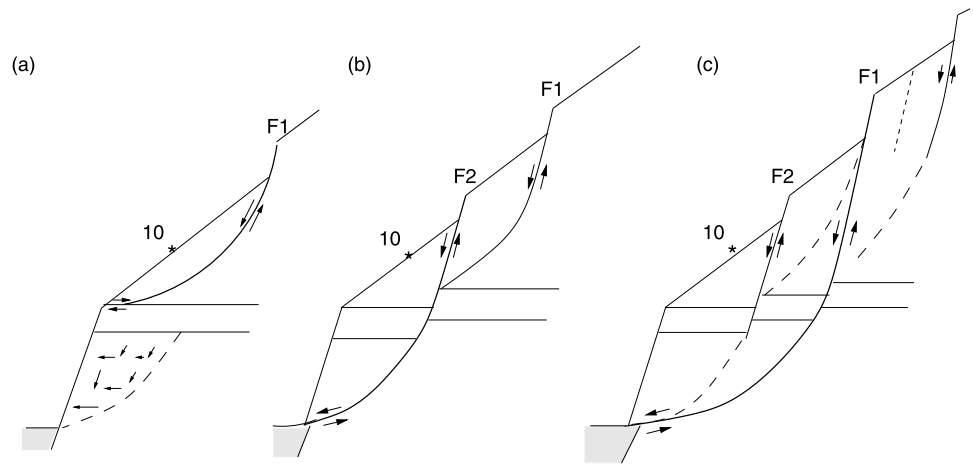

Figure 10. Schematic structural interpretation of one possible mechanism involved in the 1986–1988 crisis. The three schematic cross sections are the proposed landslide geometries (a) before 1986, (b) during the 1987 acceleration, and (c) after 1988. Follacci et al. (1993) argue for the failure of the strong gneiss bed (F2 fault) in the NW block as the driving force behind the 1986–1987 accelerating phase (Figure 10b). In the same period the development of the upper NW crack (F1 fault on the central cross section), which released the landslide from its head driving force, appears as the key parameter to slow down the accelerating slide. *Guglielmi and Vengeon* [2002] argue for all the surface faulting patterns to converge at shallow depth as listric faults that define a decollement level, which is the sliding surface. The star shows the location of bench mark 10 (adapted from *Follacci et al.* [1993]).

block reached 1780 m. This crack, which defined a new entity (that is, the upper SE block), has remained locked since then (Figures 6 and 10).

4.1.4. Current Understanding of La Clapière Acceleration

[32] On the basis of these observations and simple numerical models an interpretative model for the 1986–1988 regime change was proposed by *Follacci et al.* [1993] (for a review, see also *Susella and Zanolini* [1996]). In fact, these models do not explain the origin of the acceleration but rather try to rationalize kinematically the different changes of velocity and to rationalize why the acceleration led not to a catastrophic sliding but to a restabilization. The reasoning is based on the fact that the existing and rather strong correlation between the river flow in the valley at the bottom and the slope motion (see Figure 9) is not sufficient to explain both the destabilizing phase and the restabilization. This strongly suggests that the hydrological conditions are not the sole control parameters explaining both the strong 1986–1987 acceleration and the equally strong slowdown in 1988–1990.

[33] *Follacci et al.* [1988, 1993] argue that the failure of the strong gneiss bed in the NW block was the main driving force of the acceleration in 1986–1987. According to this view the failure of this bed induced changes in both the mechanical boundary conditions and in the local hydrogeological setting (Figure 10). Simultaneously, the development of the upper NW crack, which freed the landslide from its main driving force, appears as a key parameter to slow down the accelerating slide. The hypothesized changes in hydrological boundary conditions can further stabilize the slide after the 1986–1987 transient acceleration.

[34] Several researchers have attempted to fit the velocity time series of La Clapière landslide and to predict its future evolution using a framework similar to the Vaiont landslide discussed in section 3. The displacement of different bench marks over the 1982–1986 period has been analyzed. An exponential law has been fitted to the 1985–1986 period [*Vibert et al.*, 1988]. Using the exponential fit and a failure criterion that the landslide will collapse when the velocity reaches a given threshold, the predicted collapse time for the landslide ranges from 1988 for the NW bench mark to 1990 for the SE bench marks. Plotting the inverse of the velocity as a function of time as in equation (2) has been tried, in the hope that this law holds with $\alpha = 2$, providing a straightforward estimation of t_c. This approach applied to La Clapière velocity data predicts a collapse in 1990 for the upper NW part and in 1988–1989 for the SE part of the landslide. To remove the fluctuations of the velocity induced by changes in river flow, an ad hoc weighting of the velocity data was used by *Vibert et al.* [1988]. *Rat* [1988] stresses the importance of removing the fluctuations of the velocity induced by changes in the river flow before any attempt to predict the collapse time.

4.2. Analysis of the Cumulative Displacement and Velocity Data With the Slider Block Model

4.2.1. La Clapière Sliding Regime: 1982–1987

[35] We fit the monthly measurements of the displacement of several representative bench marks with the slider block friction model. We show results for bench mark 10, which is located in the central part of the landslide (Figure 6) and which is representative of the average landslide behavior during the 1982–1995 period (J. P. Follacci, personal communication, 2001). We have also obtained similar results for bench mark 22.

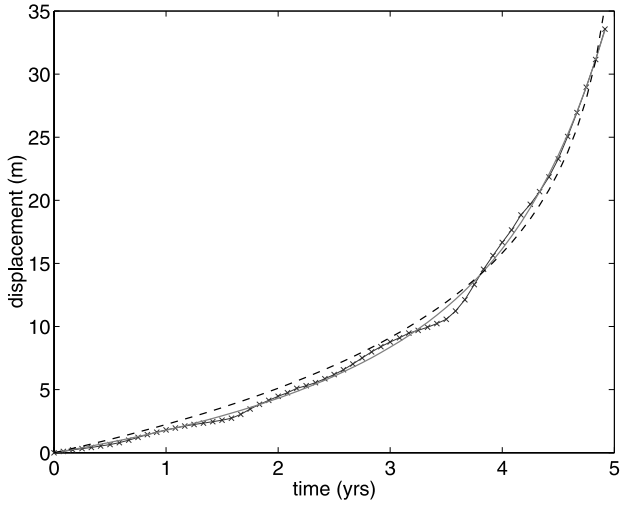

Figure 11. Displacement for bench mark 10 of La Clapière landslide (crosses) and fit using the friction model. The best fit gives $B/A = 0.999$ (thin curve). The dashed curve shows the best fit obtained when imposing $B/A = 1.5$ for comparison. See color version of this figure in the HTML.

[36] We consider only the accelerating phase in the time interval [1982.9; 1987.9]. As for the Vaiont landslide, the inversion provides the values of the parameters B/A, T, and D and the initial condition X_i of the state variable. For La Clapière we analyze the displacement as it has a lower noise level compared with the velocity. In the Vaiont case the data are of sufficiently good quality to use the velocity time series, which allows us to compare with previous studies. The best fit to the displacement of bench mark 10 is shown in Figure 11. The model parameters are $B/A = 0.999$, and the initial value of the reduced state variable is $X_i = 38$. While B/A is very close to 1, the value of X_i being significantly larger than 1 argues for La Clapière landslide to be in the stable regime (see Figure 1 and Table 1). Similar results are obtained for the other bench marks. Since the landslide underwent different regimes, it is important to perform these inversions for different time periods; that is, the fits are done from the first measurement-denoted time $t = 0$ (year 1982.9) to a later $t = t_{max}$, where t_{max} is increased from $\sim$2 years to 5 years after the initial starting date. This last time $t \approx 5$ years (end of 1987) corresponds to the time at which the slope velocity reached its peak. For all inversions except the first two points with $t_{max} \leq 2$ years, the best fit always selects an exponent $0 < B/A < 1$ and an initial state variable $X_i \gg 1$, corresponding to a stable asymptotic sliding without finite time singularity. For $t_{max} < 4$ years (that is, using data before the end of 1986) a few secondary best solutions are found with very different values, from $B/A = -3000$ to $B/A = 29$, indicating that B/A is poorly constrained. We have also performed sensitivity tests using synthetic data sets generated with the friction model with the same parameters as those obtained for La Clapière. These tests show that a precise determination of B/A is impossible but the inversion recovers the true regime $B/A < 1$.

[37] The transition time (defined by the inflection point of the velocity) is found to increase with t_{max}. The parameter X_i is also poorly constrained. Similar results are obtained for different bench marks as well as when fitting the velocity data instead of the displacement [*Helmstetter*, 2002; *Sornette et al.*, 2004]. The velocity data show large fluctuations, in part due to yearly fluctuations of the precipitation. The inversion is therefore even more unstable than the inversion of the displacement, but almost all points give $B < A$ and $X_i > 1$. Such fluctuations of the inverted solution may indicate that the use of constant friction parameters to describe a period when two regimes interact, i.e., an accelerating phase up to 1987 followed by a decrease in sliding rate since 1988, does not describe adequately the landslide behavior for the whole time period 1982–1996. The fluctuations of the model parameters may argue for a change of regime from an acceleration regime to a restabilization before the time t = 1988 of the velocity peak. Possible candidates for a change in landsliding regime include the average dip slope angle, the partitioning of blocks, new sliding surfaces, and changes in interface properties. Observed changes in morphology as suggested in Figures 6 and 10 provide evidence for changes both in driving forces and in the geometry of the landslide, including possible new sliding surfaces.

4.2.2. La Clapière Decelerating Phase: 1988–1996

[38] The simple rigid block model defined with a single block and with a velocity- and state-dependent friction law cannot account for what happened after the velocity peak without invoking additional inputs. Departure from the model prediction can be used as a guide to infer in situ landslide behavior. Recall that during the interval 1988–1990 the monthly recorded velocities slowed down to a velocity 6 times smaller than the 1987 peak values. This deceleration cannot be explained with the friction model using constant friction parameters. Indeed, for $B/A < 1$, under a constant geometry and fixed boundary conditions the velocity increases and then saturates at its maximum value. In order to explain the deceleration of the landslide, a change of material properties can be invoked (embodied, for example, in the parameter B/A), or a change of the state variable θ that describes the duration of frictional contacts, maybe due to a change in the sliding surfaces, can be invoked.

[39] We have not attempted in this study to fit both the accelerating and the decelerating phases with the slider block model because of the large number of free parameters it will imply relative to the small number of points available. Further modeling would allow block partitioning, fluctuations of the slope angle, and change with time of the friction parameters. Our purpose here is to point out how different landsliding regimes can be highlighted by the introduction of a velocity and state friction law in this basic rigid block model.

5. Discussion and Conclusion

[40] We have presented a quantitative analysis of the displacement history for two landslides, Vaiont and La Clapière, using a slider block friction model. An innovative concept proposed here was to apply to landslides the state- and velocity-dependent friction law established in the laboratory and used to model earthquake friction. Our inversion of this simple slider block friction model shows that the observed movements can be well reproduced with this simple model and suggests that the Vaiont landslide belongs to the velocity-weakening unstable regime, while La Clapière landslide should be in the strengthening stable regime. Our friction model assumes that the material properties embodied in the key parameters B/A and/or the initial value of the state variable of the friction law control the sliding regime. Even if the displacement is not homogeneous for the two landslides, the rigid block model provides a good fit to the observations and a first step toward a better understanding of the different sliding regimes and the potential for their prediction.

[41] For the cases studied here, we show that a power law increase with time of the slip velocity can be reproduced by a rigid slider block model. This first-order model rationalizes the previous empirical law suggested by *Voight* [1988b]. Following *Petley et al.* [2002], we suggest that the landslide power law acceleration emerges in the presence of a rigid block; that is, this corresponds to the slide of a relatively stiff material. *Petley et al.* [2002] report that for some other types of landslides in ductile material the slips do not follow a linear dependence with time of the inverse landslide velocities. They suggest that the latter cases are reminiscent of the signature of landsliding associated with a ductile failure in which crack growth does not occur. In contrast, they propose that the linear dependence of the inverse velocity of the landslide as a function of time is reminiscent of crack propagation, i.e., brittle deformation on the basal shear plane. Our contribution suggests that friction is another possible process that can reproduce the same accelerating pattern as crack growth on a basal shear plane [*Petley et al.*, 2002; *Kilburn and Petley*, 2003]. The friction model used in our study requires the existence of an interface. Whether this friction law should change for ductile material is not clear. The lack of direct observations of the shearing zone and its evolution through time makes the task of choosing between the two classes of models, crack growth versus state- and velocity-dependent friction, difficult.

[42] For La Clapière landslide the inversion of the displacement data for the accelerating phase 1982–1987 up to the maximum velocity gives $B/A < 1$, corresponding to the stable regime. The deceleration observed after 1988 implies that not only is La Clapière landslide in the stable regime but, in addition, some parameters of the friction law have changed, resulting in a change of sliding regime from a stable regime to one characterized by a smaller velocity, as if some stabilizing process or reduction in stress was occurring. The major innovation of the frictional slider block model, which is explored further by *Sornette et al.* [2004], is to embody the two regimes (stable versus unstable) in the same physically based framework and to offer a way of distinguishing empirically between the two regimes, as shown by our analysis of the two cases provided by the Vaiont and La Clapière landslides.

Appendix A: Derivation of the Full Solution of the Frictional Problem

[43] We now provide the full solution of the frictional problem. First, we rewrite equation (3) as

$$\dot{\delta} = SD_c \left(\frac{\theta}{\theta_0}\right)^{-B/A}, \tag{A1}$$

where

$$S \equiv \frac{\dot{\delta}_0 \exp\left[\frac{\tau}{\sigma}-\mu_0\right]}{D_c}. \quad (A2)$$

Putting equation (A1) in equation (4) gives

$$\frac{d(\theta/\theta_0)}{dt} = \frac{1}{\theta_0} - S(\theta/\theta_0)^{1-B/A}. \quad (A3)$$

The case $B = A$ requires special treatment since the dependence in θ disappears in the right-hand side of equation (A3) and $d\theta/dt$ is constant.

[44] For $B/A \neq 1$ it is convenient to introduce the reduced variables

$$X \equiv (S\theta_0)^{1/(1-B/A)} \frac{\theta}{\theta_0} \quad (A4)$$

$$D \equiv D_c \left(S\theta_0^B/A\right)^{1/(1-B/A)}. \quad (A5)$$

Then equation (A1) reads

$$\dot{\delta} = DX^{-B/A}. \quad (A6)$$

Putting equation (A1) in equation (4) to eliminate the dependence in $\dot{\delta}$, we obtain

$$\frac{dX}{dt'} = 1 - X^{1-B/A}, \quad (A7)$$

where $t' = t/T$ with

$$T = \frac{D_c}{D} = \left[\frac{D_c}{\dot{\delta}_0 \theta_0^{B/A}}\right]^{1/(1-B/A)} \exp\left[\frac{(\tau/\sigma)-\mu_0}{(B-A)}\right]. \quad (A8)$$

We shall drop the prime and use the dimensionless time t, meaning that time is expressed in units of T except where stated otherwise. Note that equation (A7) is nothing but a dimensionless reformulation of equation (A3). Equation (A3) itself comes from equations (3) and (4), which are the fundamental equations describing the rate- and state-dependent friction, with the additional simple ingredient that the friction coefficient is constant and equal to the ratio of the shear over normal stress (assumed to be constant because of the fixed geometry of the block).

[45] The block sliding behavior is determined by first solving equation (A7) for the normalized state variable $X(t)$ and then inserting this solution in equation (A6) to get the slip velocity. Equation (A7) displays different regimes as a function of B/A and of the initial value X_i compared with 1 that we now classify.

A1. Case $B/A > 1$

[46] For $B > A$ and $X_i < 1$ the initial rate of change dX/dt of the state variable is negative. The initial decay of X accelerates with time, and X reaches 0 in finite time. Expression (A6) shows that $\delta(t)$ continuously accelerates and reaches infinity in finite time. The divergence is, of course, unrealistic for landslides; it simply signals a bifurcation from accelerated creep to complete slope instability for which inertia is no longer negligible.

[47] Close to the critical time we can neglect the first term 1 in the right-hand side of equation (A7), and we recover the asymptotic solution (equations (9), (10), and (11)):

$$X(t) \simeq \left(\frac{B}{A}\right)^{A/B} (t_c - t)^{A/B}, \quad (A9)$$

where the critical time t_c is determined by the initial condition $X(t = 0) = X_i$:

$$t_c = \frac{X_i^{B/A} A}{B}. \quad (A10)$$

[48] For $B > A$ and $X_i > 1$ the initial rate of change dX/dt of the state variable is positive; thus X increases initially. This growth goes on, fed by the positive feedback embodied in equation (A7). At large times, X increases asymptotically at the constant rate dX/dt, leading to $X(t) \approx t$. Integrating equation (A6) gives

$$\delta(t) = \delta_\infty - \frac{\dot{\delta}_0 D}{B/A - 1} \frac{1}{t^{(B/A)-1}} \quad (A11)$$

at large times. The asymptotic value of the displacement δ_∞ is determined by the initial condition. This regime thus describes a decelerating slip slowing down as an inverse power of time. It corresponds not to a destabilizing landslide but to a power law plasticity hardening.

A2. Case $B = A$

[49] In this case the variables (A4) and (A5) are not defined, and we go back to equation (4) (which uses the unnormalized state variable θ and time t) to obtain

$$\frac{d\theta}{dt} = 1 - S\theta_0, \quad (A12)$$

where S is defined by equation (A2) and depends on the material properties but not on the initial conditions. If $S\theta_0 > 1$, θ decays linearly and reaches 0 in finite time. This retrieves the finite time singularity, with the slip velocity diverging as $1/(t_c - t)$ corresponding to a logarithmic singularity of the cumulative slip. If $S\theta_0 < 1$, θ increases linearly with time. As a consequence, the slip velocity decays as $\dot{\delta} \sim 1/t$ at large times, and the cumulative slip grows asymptotically logarithmically as $\ln t$. This corresponds to a standard plastic hardening behavior.

A3. Case $B < A$

[50] For $X_i > 1$ the initial rate of change dX/dt of the state variable is negative; thus X decreases and converges on the stable fixed point $X = 1$ exponentially as

$$X = 1 + ae^{-t/t^*}, \quad (A13)$$

where the relaxation time t^* is given by

$$t^* = \frac{1}{1 - B/A} \quad (A14)$$

in units of T and a is a constant determined by the initial condition. The case $B/A < 0$ can be observed as B can be negative, as found by *Blanpied et al.* [1995]. This rather special case corresponds to a friction coefficient decreasing with the increase of the surface of contacts. Starting from some initial value, the slip velocity increases for $0 < B/A < 1$ (decreases for $B/A < 0$) and converges to a constant value according to equations (A1) and (A6).

[51] For $X_i < 1$ the initial rate of change dX/dt of the state variable is positive, and X converges exponentially toward the asymptotic stable fixed point $X = 1$. As θ increases toward a fixed value, this implies that the slip velocity decreases for $0 < B/A < 1$ (increases for $B/A < 0$) toward a constant value.

[52] **Acknowledgments.** We thank C. Scavia and Y. Guglielmi for key support in capturing archive data for the Vaiont and La Clapière landslides, respectively. We are very grateful to N. Beeler, J. Dieterich, Y. Guglielmi, D. Keefer, J. P. Follacci, and J. M. Vengeon for useful suggestions and discussions. A.H. and J.R.G. were supported by INSU French grants, Gravitational Instability ACI. S.G. and D.S. acknowledge support from the James S. McDonnell Foundation 21st Century Scientist award/Studying Complex Systems.

References

Anifrani, J.-C., C. Le Floch, D. Sornette, and B. Souillard (1995), Universal log-periodic correction to renormalization group scaling for rupture stress prediction from acoustic emissions, *J. Phys. I*, *5*, 631–638.

Bhandari, R. K. (1988), Some lessons in the investigation and field monitoring of landslides, in *Proceedings of the 5th International Symposium on Landslides*, vol. 3, edited by C. Bonnard, pp. 1435–1457, A. A. Balkema, Brookfield, Vt.

Blanpied, M. L., D. A. Lockner, and J. D. Byerlee (1995), Frictional slip of granite at hydrothermal conditions, *J. Geophys. Res.*, *100*, 13,045–13,064.

Broili, L. (1967), New knowledge on the geomorphology of the Vaiont slide slip surfaces, *Rock Mech.*, *5*, 38–88.

Campbell, C. S. (1989), Self-lubrication for long runout landslides, *J. Geol.*, *97*, 653–665.

Caplan-Auerbach, J., C. G. Fox, and F. K. Duennebier (2001), Hydroacoustic detection of submarine landslides on Kilauea volcano, *Geophys. Res. Lett.*, *28*, 1811–1813.

Centre Etudes Techniques de l'Equipement (CETE) (1996), Base de donnees glissement de Laclapiere, database, Nice, France.

Centre Etudes Techniques de l'Equipement (CETE) (1999), Base de donnees glissement de Laclapiere, database, Nice, France.

Chau, K. T. (1995), Landslides modeled as bifurcations of creeping slopes with nonlinear friction law, *Int. J. Solids Struct.*, *32*, 3451–3464.

Chau, K. T. (1999), Onset of natural terrain landslides modelled by linear stability analysis of creeping slopes with a two state friction law, *Int. J. Numer. Anal. Methods Geomech.*, *23*, 1835–1855.

David, E. (2000), Glissement de la Clapière, St. Etienne de Tinée, Etude cinématique, géomorphologique et de stabilité, *rapp.*, 88 pp., ATM-Cent. Etud. Tech de l'Equip., Nice, France.

Davis, R. O., N. R. Smith, and G. Salt (1990), Pore fluid frictional heating and stability of creeping landslides, *Int. J. Numer. Anal. Methods Geomech.*, *14*, 427–443.

Dieterich, J. (1978), Time dependent friction and the mechanics of stick slip, *Pure Appl. Geophys.*, *116*, 790–806.

Dieterich, J. H. (1992), Earthquake nucleation on faults with rate- and state-dependent strength, *Tectonophysics*, *211*, 115–134.

Durville, J. L. (1992), Study of mechanisms and modeling of large slope movements, *Bull. Int. Assoc. Eng. Geol.*, *45*, 25–42.

Eisbacher, G. H. (1979), Cliff collapse and rock avalanches in the Mackenzie Mountains, Northwestern Canada, *Can. Geotech. J.*, *16*, 309–334.

Erismann, T. H., and G. Abele (2000), *Dynamics of Rockslides and Rockfalls*, 300 pp., Springer-Verlag, New York.

Follacci, J. P. (2000), Photographic album of La Clapière landslide, database, Cent. Etud. Tech. de l'Equip., Nice, France.

Follacci, J. P., P. Guardia, and J. P. Ivaldi (1988), La Clapière landslide in its geodynamical setting, in *Proceedings of the 5th International Symposium on Landslides*, vol. 3, edited by C. Bonnard, pp. 1323–1327, A. A. Balkema, Brookfield, Vt.

Follacci, J.-P., L. Rochet, and J.-F. Serratrice (1993), Glissement de La Clapière, St. Etienne de Tinée, Synthèse des connaissances et actualisation des risques, *rapp. 92/PP/UN/I/DRM/03/AI/01*, 76 pp., Cent. Etud. Tech. de l'Equip., Nice, France.

Fruneau, B., J. Achache, and C. Delacourt (1996), Observation and modeling of the Saint-Etienne-de-Tinée landslide using SAR interferometry, *Tectonophysics*, *265*, 181–190.

Fukuzono, T. (1985), Method for predicting the failure time of a slope, paper presented at 3rd International Conference Field Workshop on Landslides, Natl. Res. Cent. for Disaster Prev., Tokyo.

Gluzman, S., and D. Sornette (2001), Self-consistent theory of rupture by progressive diffuse damage, *Phys. Rev. E*, *63*, 066,129.

Gomberg, J., P. Bodin, W. Savage, and M. E. Jackson (1995), Landslide faults and tectonic faults, Analogs?—The slumgullion earthflow, Colorado, *Geology*, *23*, 41–44.

Gomberg, J., N. Beeler, and M. Blanpied (2000), On rate-state and Coulomb failure models, *J. Geophys. Res.*, *105*, 7857–7871.

Guglielmi, Y., J. M. Vengeon, C. Bertrand, J. Mudry, J. P. Follacci, and A. Giraud (2002), Hydrogeochemistry: An investigation tool to evaluate infiltration into large moving rock masses (case study of La Clapière and Sechilienne alpine landslides), *Bull. Eng. Geol. Environ.*, *61*(4), 311–324.

Heim, A. (1932), *Bergsturz und Menschenleben*, 218 pp., Fretz and Wasmuth, Zurich, Switzerland.

Helmstetter, H. (2002), Rupture and instabilities: Seismicity and landslides, Ph.D. thesis, 387 pp., Grenoble Univ., Grenoble, France.

Hendron, A. J., and F. D. Patton (1985), The Vaiont slide, a geotechnical analysis based on new geologic observations of the failure surface, *Tech. Rep. GL-85-5*, vols. I and II, U.S. Army Eng. Waterways Exp. Stn., Vicksburg, Miss.

Hoek, E., and J. W. Bray (1997), *Rock Slope Engineering*, 3rd ed., 358 pp., Inst. of Min. and Metal., London.

Hoek, E., and E. T. Brown (1980), *Underground Excavation in Rock*, Inst. of Min. and Metal., London.

Jaume, S. C., and L. R. Sykes (1999), Evolving toward a critical point: A review of accelerating seismic moment/energy release prior to large and great earthquakes, *Pure Appl. Geophys.*, *155*, 279–305.

Kennedy, B. A., and K. E. Niermeyer (1971), Slope monitoring systems used in the prediction of a major slope failure at the Chuquicamata mine, Chile, in *Proceedings on Planning Open Pit Mines*, pp. 215–225, A. A. Balkema, Brookfield, Vt.

Kilburn, C. R. J., and D. N. Petley (2003), Forecasting giant, catastrophic slop collapse: Lessons from Vajont, northern Italy, *Geomorphology*, *54*, 21–32.

Korner, J. H. (1976), The reach and velocity of catastrophic landslides and flowing snow avalanches, *Rock Mech.*, *8*, 225–236.

Malet, J. P., O. Maquaire, and E. Calais (2002), The use of global positioning system techniques for the continuous monitoring of landslides: Application to the Super-Sauze earthflow (Alpes-de-Haute-Provence, France), *Geomorphology*, *43*, 33–54.

Mantovani, F., R. Soeters, and C. J. Vanwesten (1996), Remote sensing techniques for landslide studies and hazard zonation in Europe, *Geomorphology*, *15*, 213–225.

Marone, C. (1998), Laboratory-derived friction laws and their application to seismic faulting, *Annu. Rev. Earth Planet. Sci.*, *26*, 643–696.

Muller, L. (1964), The rock slide in the Vaiont valley, *Felsmech. Ingenoirgeol.*, *2*, 148–212.

Muller, L. (1968), New considerations on the Vaiont slide, *Felsmech. Ingenoirgeol.*, *6*, 1–91.

Parise, M. (2001), Landslide mapping techniques and their use in the assessment of the landslide hazard, *Phys. Chem. Earth, Part C*, *26*, 697–703.

Petley, D. N., M. H. Bulmer, and W. Murphy (2002), Patterns of movement in rotational and translational landslides, *Geology*, *30*(8), 719–722.

Rabotnov, Y. N.(1969), *Creep Problems in Structural Members*, North-Holland, New York.

Rat, M. (1988), Difficulties in forseeing failure in landslides—La Clapière, French Alps, in *Proceedings of the 5th International Symposium on Landslides*, vol. 3, edited by C. Bonnard, pp. 1503–1504, A. A. Balkema, Brookfield, Vt.

Rousseau, N. (1999), Study of seismic signals associated with rockfalls at 2 sites on the Reunion Island (Mahavel Cascade and Souffrière cavity), Ph.D. thesis, Inst. de Phys. du Globe de Paris, Paris.

Ruina, A. (1983), Slip instability and state variable friction laws, *J. Geophys. Res.*, *88*, 10,359–10,370.

Saito, M. (1965), Forecasting the time of occurrence of a slope failure, *Proc. Int. Conf. Soil Mech. Found. Eng., 6th*, vol. 2, 537–541.

Saito, M. (1969), Forecasting time of slope failure by tertiary creep, *Proc. Int. Conf. Soil Mech. Found. Eng., 7th*, vol. 2, 677–683.

Saito, M., and H. Uezawa (1961), Failure of soil due to creep, *Proc. Int. Conf. Soil Mech. Found. Eng., 6th*, vol. 1, 315–318.

Sammis, S. G., and D. Sornette (2002), Positive feedback, memory and the predictability of earthquakes, *Proc. Natl. Acad. Sci. U.S.A.*, *99*, 2501–2508.

Scholz, C. H. (1990), *The Mechanics of Earthquakes and Faulting*, Cambridge Univ. Press, New York.
Scholz, C. H. (1998), Earthquakes and friction laws, *Nature*, *391*, 37–42.
Sornette, D., and C. G. Sammis (1995), Complex critical exponents from renormalization group theory of earthquakes: Implications for earthquake predictions, *J. Phys. I*, *5*, 607–619.
Sornette, D., A. Helmstetter, J. V. Andersen, S. Gluzman, J.-R. Grasso, and V. Pisarenko (2004), Towards landslide predictions: Two case studies, *Physica A*, in press.
Susella, G., and F. Zanolini (Eds.) (1996), Risques générés par les grands mouvements de terrains, report, 207 pp., Univ. Joseph Fourier, Grenoble, France.
Van Asch, T. W. J., J. Buma, and L. P. H. Van Beek (1999), A view on some hydrological triggering systems in landslides, *Geomorphology*, *30*, 25–32.
Vangenuchten, P. M. B., and H. Derijke (1989), Pore water pressure variations causing slide velocities and accelerations observed in a seasonally active landslide, *Earth Surf. Processes Landforms*, *14*, 577–586.
Vibert, C., M. Arnould, R. Cojean, and J. M. Cleac'h (1988), An attempt to predict the failure of a mountainous slope at St. Etienne de Tinée, France, in *Proceedings of the 5th International Symposium on Landslides*, vol. 2, edited by C. Bonnard, pp. 789–792, A. A. Balkema, Brookfield, Vt.
Voight, B. (Ed.) (1978), *Rockslides and Avalances*, vol. 2, *Engineering Sites*, *Dev. Geotech. Eng.*, vol. 14B, pp. 595–632, Elsevier Sci., New York.
Voight, B. (1988a), A method for prediction of volcanic eruption, *Nature*, *332*, 125–130.
Voight, B. (1988b), Materials science laws applied to time forecast of slope failure, in *Proceedings of the 5th International Symposium on Landslides*, vol. 3, edited by C. Bonnard, pp. 1471–1472, A. A. Balkema, Brookfield, Vt.
Voight, B. A. (1989), A relation to describe rate-dependent material failure, *Science*, *243*, 200–203.
Xu, Z. Y., S. Y. Schwartz, and T. Lay (1996), Seismic wave-field observations at a dense small-aperture array located on a landslide in the Santa Cruz Mountains, California, *Bull. Seismol. Soc. Am.*, *86*, 655–669.

J. V. Andersen, U. F. R. de Sciences Economiques, Gestion, Mathématiques et Informatique, CNRS UMR7536 and Université Paris X-Nanterre, F-92001 Nanterre Cedex, France. (vitting@unice.fr)

S. Gluzman, A. Helmstetter, and D. Sornette, Institute of Geophysics and Planetary Physics, University of California, Los Angeles, CA 90095-1567, USA. (simon.gluzman@generation5.net; helmstet@moho.ess.ucla.edu; sornette@moho.ess.ucla.edu)

J.-R. Grasso, U.S. Geological Survey, 345 Middlefield Road MS 977, Menlo Park, CA 94025-3591, USA. (jean-robert.grasso@obs.ujf-grenoble.fr)

V. Pisarenko, International Institute of Earthquake Prediction Theory and Mathematical Geophysics, Russian Ac. Sci., Warshavskoye sh., 79, kor. 2, Moscow 113556, Russia. (pisarenko@yaol.ru)